REVISED Supporting Information
For article to *Nanoscale*, RSC publisher

The functionalization of nanodiamonds *(diamondoids)* as key parameter of their easily controlled self-assembly in micro- and nanocrystals from vapor phase

Maria A. Gunawan, Didier Poinsot, Bruno Domenichini, Céline Dirand, Sébastien Chevalier, Andrey A. Fokin, Peter Schreiner and Jean-Cyrille Hierso

---

Content

1. General conditions ……p.3

2. Vapor Pressure Measurements of Diamondoids and Thermodynamic Data ……p.3

a. Adamantane ……p.8

b. Diamantane ……p.9

c. 1-Hydroxydiamantane ……p.10

d. 4-Hydroxydiamantane ……p.11

e. 4-Fluorodiamantane ……p.12

3. Vapor Deposition Conditions and Apparatus ……p.13

a. Deposition at atmospheric pressure or low vacuum ……p.13

b. Vapor deposition apparatus for experiments under high vacuum (PVD) ……p.14

XPS and EDX data ……p.16

4. Optical Microscopy of Deposits from Vapor Deposition of Diamondoids ……p.18

a. Adamantane ……p.18

b. 1–Hydroxyadamantane ……p.18

c. Adamantyl diphenylphosphinite ……p.19

d. Aminoadamantane ……p.19

e. Diamantane ……p.19

f. 1-Hydroxydiamantane ……p.20

g. 4-Hydroxydiamantane ……p.21

h. 4,9-Dihydroxydiamantane ……p.21

i. 4-Fluorodiamantane ……p.21

j. 4,9-Difluorodiamantane ……p.22

5. Control of crystallinity from X-Ray diffraction ……p.23

6. Deposits from Solution Dip Coating of Functionalized Diamondoids ……p.24

References ……p.25

1) General Conditions

Pristine adamantane and diamantane were prepared in the Giessen group and were purified by sublimation before use. 1-Aminoadamantane and 1-hydroxyadamantane were obtained from Alfa Aesar and Aldrich. 1-Hydroxydiamantane, 4-hydroxydiamantane, and 4,9-dihydroxydiamantane were synthesized from diamantane *[Eur. J. Org. Chem. 2007, 4738-4745*]; 4-fluorodiamantane and 4,9-difluorodiamantane were prepared from its hydroxyl derivatives [*Adv. Synth. Catal. 2009, 351, 1041-1054*]. The melting points reported for diamondoids were measured by DSC TA instrument 2920 Modulated, with a temperature calibrated by an Indium reference and at heat of 10 °C/min under nitrogen flow.

2) Vapor Pressure Measurements of Diamondoids and Thermodynamic Data

Measurements of sublimation enthalpies can be based on mass transport, and as such they are directly related to vapor pressure. The studies previously reported on enthalpy of sublimation of diamondoids can give markedly different values, depending on the measurement modes or the methods of calculation; this is exemplified for diamantane in **Table 1S**.

Table 1S: Sublimation Enthalpy of Diamantane Reported in the Literature

ΔH_{sub} (kJ mol^{-1})	Methods of determination	Ref.
117.2 ± 8	Sum of enthalpies of vaporization and fusion measured by calorimetry using bomb combustion	[1,2]
74.9	First-order calculation of the molecular-rotation potential	[3]
95.96 ± 0.80	Gas-saturation temperature scanning using gas chromatography	[4]
95.94 ± 0.80	Calorimetry using bomb combustion	[5]
73.5 and 82.8	DFT calculations from the molecular surface properties	[6]

In order to accurately measure the vapor pressure of finely divided diamondoid powders a system inspired by the method used for measuring the vapor pressure of liquids at liquid-vapor equilibrium state was developed (**Figure 1S$_{a,b}$**).

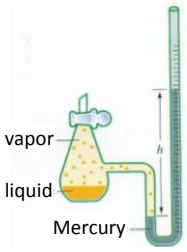

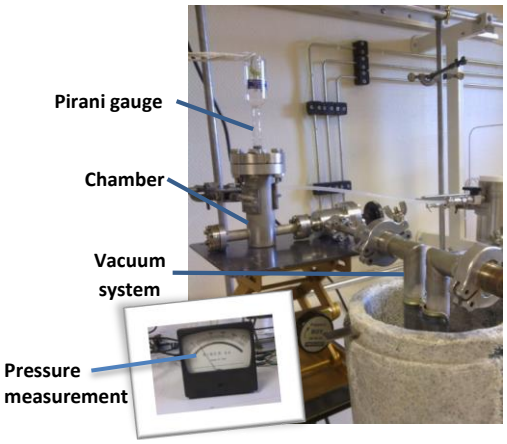

Figure 1S$_a$: General method for the measurements of liquid vapor pressure

Figure 1S$_b$: Experimental setup for measurement of functionalized diamandoids vapor pressures

A closed sublimation chamber connected with a calibrated Pirani gauge was used, which allows measuring the vapor pressure for diamondoid reaching its solid-vapor equilibrium state at a given temperature. The whole system is made of temperature-resistant glass and metal pieces, including the Pirani gauge, the joints, and gauge cable. For degasing and cleaning purpose this sublimation chamber was rinsed with ethanol then heated in an oven at a temperature over 70 °C for >5 h while connected to a vacuum pump protected by a cold trap using liquid nitrogen. The oven was also conditioned at a given temperature for 16 h before use, for insuring a homogeneous and stable temperature. The purity of synthesized diamondoids was verified by GC-MS. Adamantane, diamantane and naphthalene were purified by sublimation. Diamondoids (about 300 mg) were grinded before being placed into a small glass flacon and weighted with a precision balance. The sample was put inside the sublimation chamber which was connected with a calibrated Pirani gauge (precision ±1µmHg, ±0.13 Pa). To dry the diamondoids powder, four cycles of primary vacuum / heating at 70 °C / cooling at room temperature were applied before measurements. Then, the chamber was put under vacuum during 5 minutes, to reach the lowest pressure (*caution* this value varies with the type of diamondoid, for example adamantane 100-118 µmHg, diamantane 11.5–15 µmHg, and naphthalene 90–181 µmHg). A valve positioned between the chamber and vacuum

system was closed. After the chamber was disconnected from the vacuum system, it was put inside the oven that has been set up at a specific temperature (for instance 60 °C) and the pressure inside the chamber was measured with a manometer until it reached an equilibrium state (usually every 1 to 5 min, and then every hour, during 8 h). The entire system, the chamber and the measuring gauge were placed inside the oven. The temperature of the oven was controlled with a thermocouple connected to a multimeter. The thermocouple was calibrated by measuring boiling point of distilled water and melting point of ice. Comparing these values with its theoretical boiling point and melting point at local pressure (local pressure data was recorded from Dijon's official national Weather Station).

The pressure was measured with a manometer in the scale 0–1000 µmHg. This method was repeated for various temperatures ranging from 20 to 75 °C. For room temperature, the system was placed in the oven turned-off.

Accurate calibration of the Pirani gauge was done with an appropriate standard product of known vapor pressure. Naphthalene was used for calibration of the gauge for temperature between 20 and 55 °C, because of technical limitation an exponential extrapolation was operated for temperatures between 55 and 75 °C with r^2 fitting > 0.999. Vapor pressures of naphthalene measured at different temperatures with our system are given in **Figure 2S**.

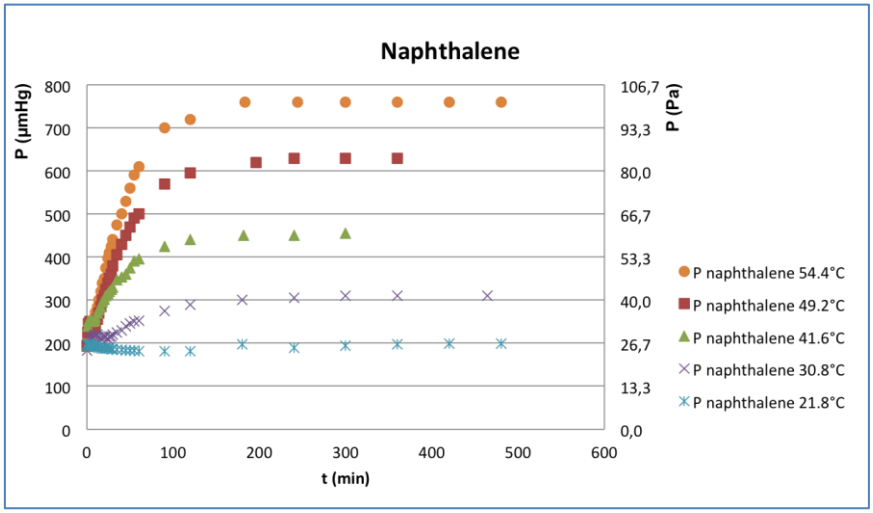

Figure 2S. Monitoring of naphtalene vapor pressure at various temperatures

Calibration of the gauge as a function of the temperature was achieved by calculating the invert ratio of the vapor pressure of naphthalene that was measured at equilibrium state (**Figure 3S**, after 4 h experiments) over the reported references values (**Figure 4S**),[7] as reported in **Table 2S**.

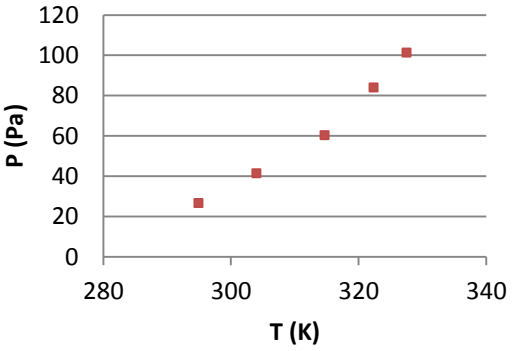

Figure 3S. Saturated vapor pressure of naphtalene as a function of temperature

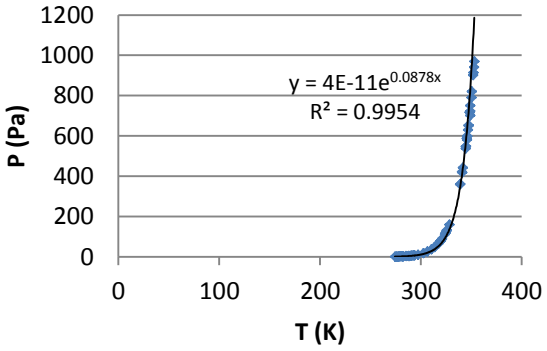

Figure 4S. Saturated vapor pressure of naphtalene from literature data

Table 2S: Calibration of the Pirani gauge from naphthalene measurement and ref. [7]

T_{exp} (°C)	T_{exp} (K)	P_{ref} (Pa)	P_{exp} (Pa)	P_{ref} / P_{exp} ratio
54.40	327.55	123.5627	101.3080	1.2197
49.20	322.35	78.2719	83.9790	0.9320
41.55	314.70	39.9856	60.2072	0.6641
30.85	304.00	15.6279	41.3230	0.3782
21.80	294.95	7.0602	26.5267	0.2662

The calibration curve in **Figure 5S** was obtained by plotting [P_{ref} / P_{exp} ratio] as a function of the temperature [T] (K).

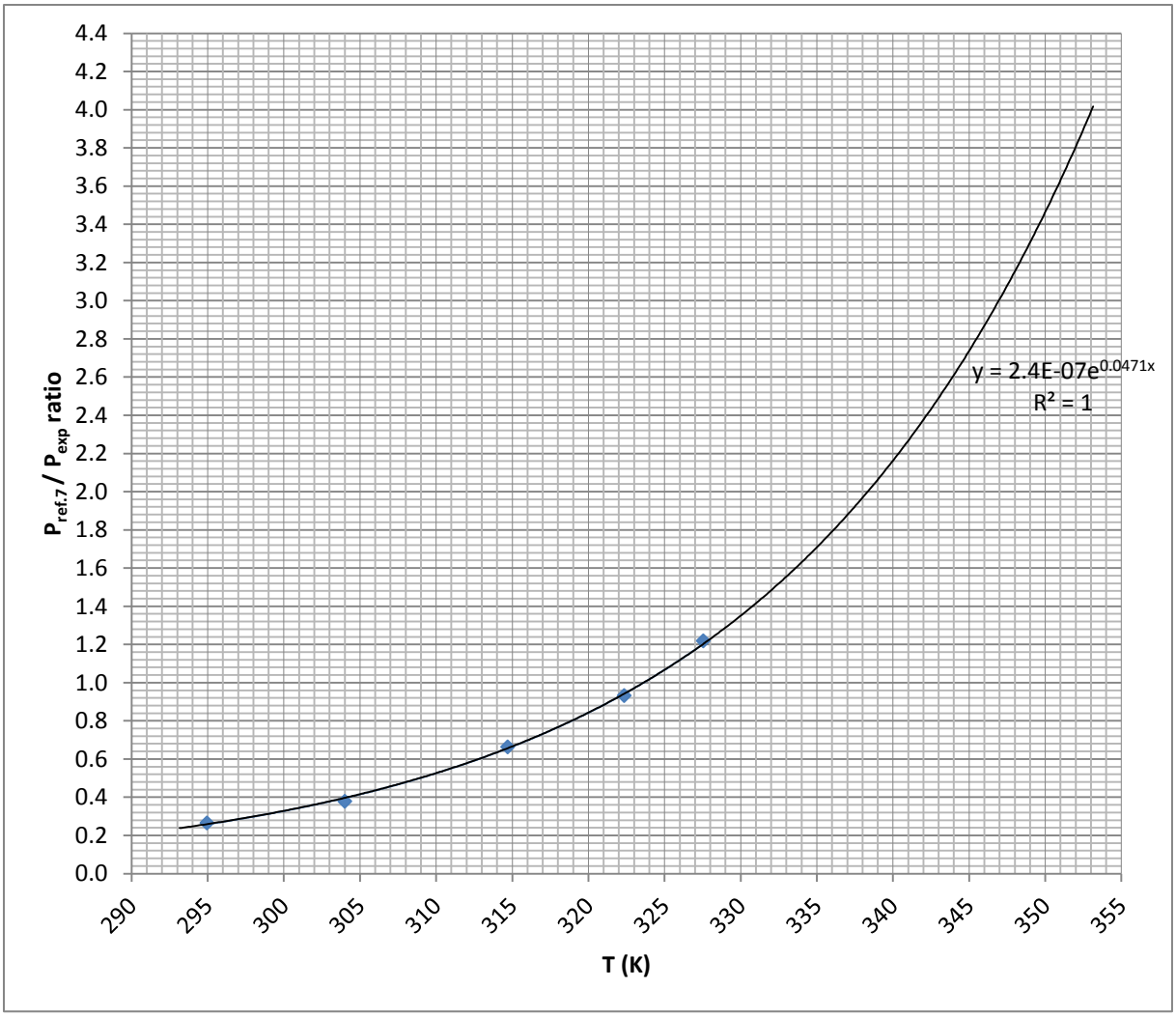

Figure 5S. Naphtalene vapor pressure calibration curve.

The calibration curve in **Figure 5S** was used to calculate the vapor pressure of diamondoids from our measurements by correction of the pressure ratio for a given temperature. This is illustrated below for five different diamondoids: adamantane, diamantane, 1-hydroxydiamantane, 4-hydroxydiamantane, and 4-fluorodiamantane.

a) Adamantane

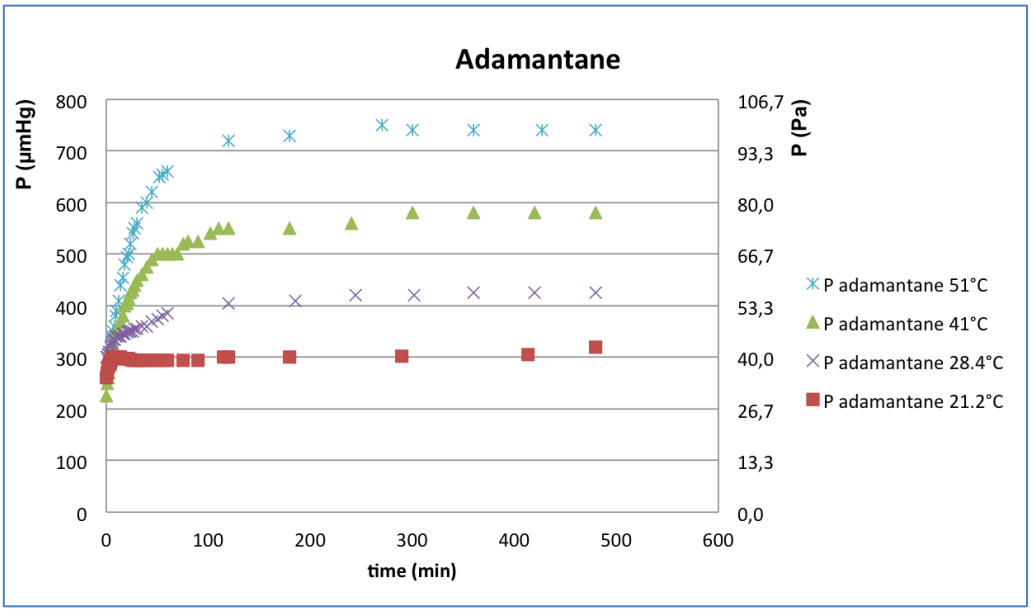

Figure 6S. Vapor pressure measurement for adamantane

Table 3S: Experimental vapor pressure and corrections for adamantane

T_{exp} (K)	P_{exp} (Pa)	P_{ref}/P ratio	$P_{corrected}$	1/T	ln ($P_{corrected}$)
294.38	41.1897	0.2523	**10.3918**	$3.397.10^{-3}$	2.3410
301.58	56.4859	0.3540	**19.9963**	$3.316.10^{-3}$	2.9955
314.18	77.3140	0.6408	**49.5455**	$3.183.10^{-3}$	3.9029
324.23	98.6420	1.0288	**101.4806**	$3.084.10^{-3}$	4.6199

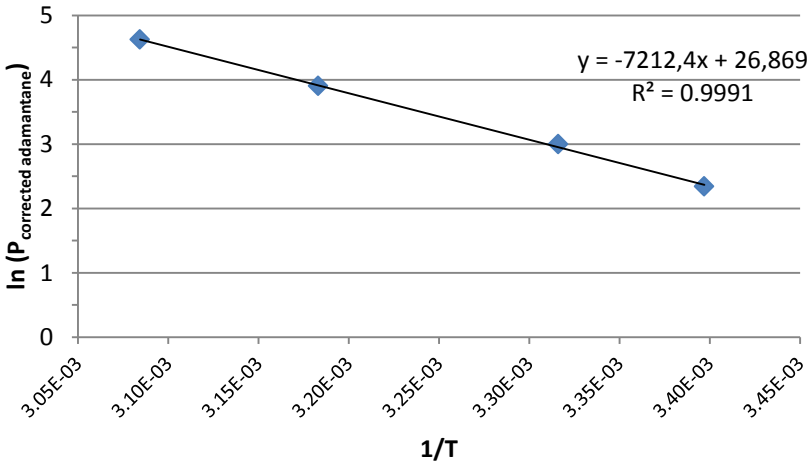

Figure 7S. Clausius-Clapeyron plot for adamantane

Clausius-Clapeyron equation allows determining ΔH:

$$\ln P = -\frac{\Delta H^{sv}}{R}\frac{1}{T} + \left(\frac{\Delta S^{sv}}{R}\right)$$

The enthalpy of sublimation of adamantane is ΔH = **60.0** ± **5** kJ/mol.

b) <u>Diamantane</u>

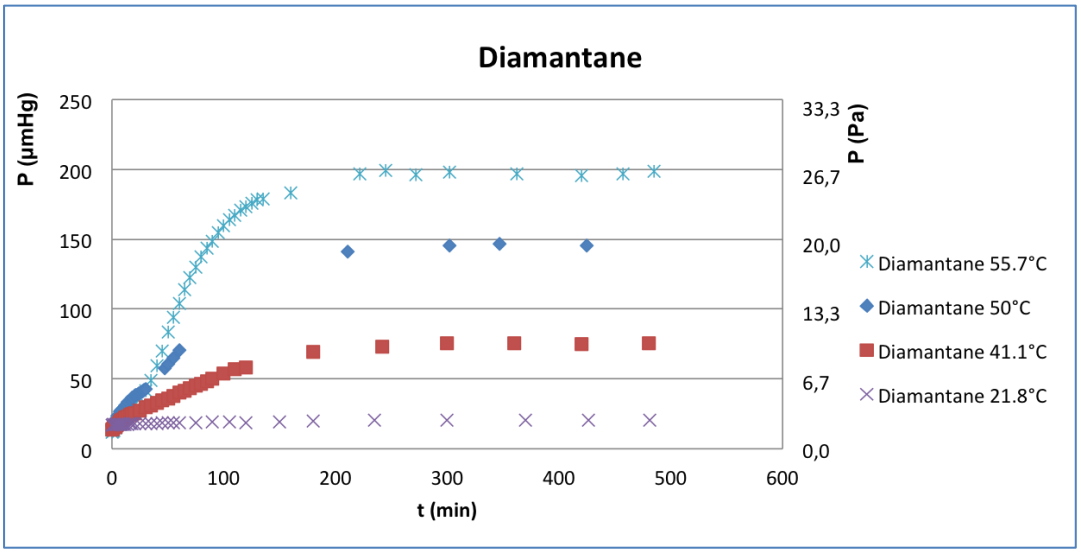

Figure 8S. Vapor pressure measurement for diamantane

Table 4S: Experimental vapor pressure and corrections for diamantane

T_{exp} (K)	P_{exp} (Pa)	P_{ref}/P ratio	$P_{corrected}$	1/T	ln ($P_{corrected}$)
294.98	2.7365	0.2594	**0.7099**	$3.390.10^{-3}$	-0.3426
314.28	10.0508	0.6439	**6.4713**	$3.182.10^{-3}$	1.8674
323.18	19.4391	0.9795	**19.0410**	$3.094.10^{-3}$	2.9466
328.89	26.2774	1.2816	**33.6765**	$3.041.10^{-3}$	3.5168

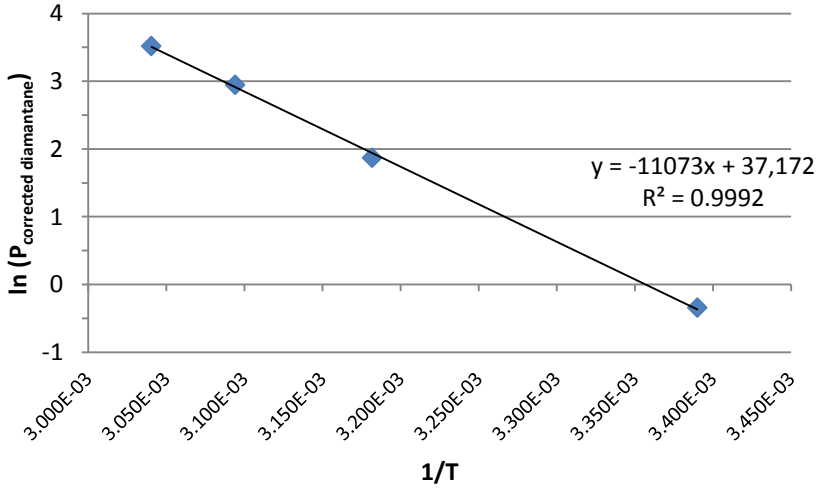

Figure 9S. Clausius-Clapeyron plot for diamantane

The enthalpy of sublimation of diamantane is ΔH = **92.1 ± 5** kJ/mol.

c) <u>1-Hydroxydiamantane</u>

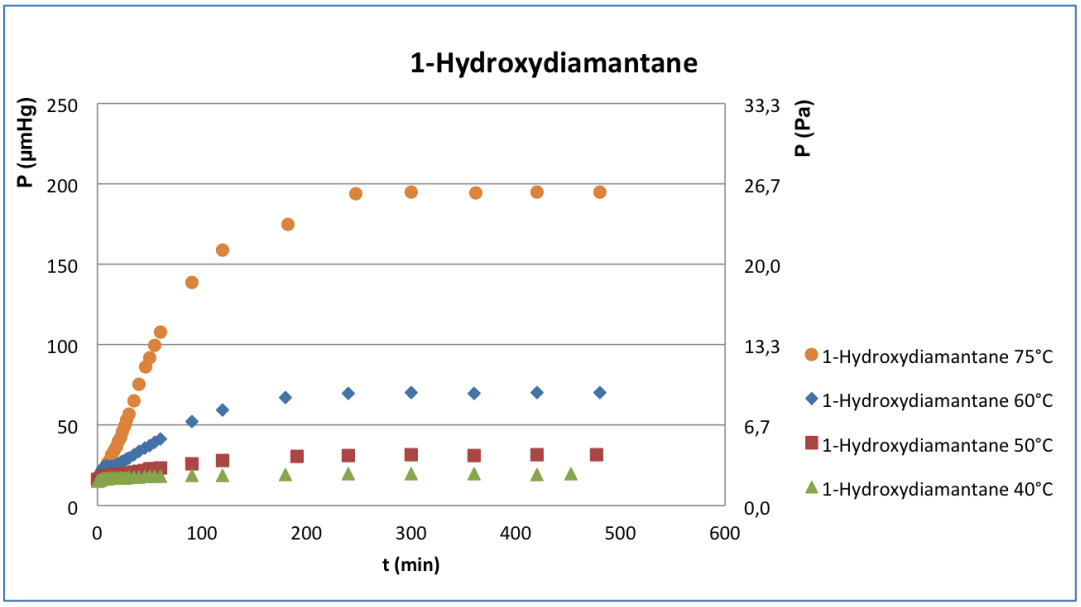

Figure 10S. Vapor pressure measurement for 1-hydroxydiamantane

Table 5S: Experimental vapor pressure and corrections for 1-hydroxydiamantane

T_{exp} (K)	P_{exp} (Pa)	P_{ref}/P ratio	$P_{corrected}$	1/T	ln ($P_{corrected}$)
313.00	2.6139	0.6063	**1.5849**	$3.195.10^{-3}$	0.4605
322.60	4.1892	0.9530	**3.9922**	$3.100.10^{-3}$	1.3843
333.20	9.3577	1.5700	**14.6918**	$3.001.10^{-3}$	2.6873
348.85	25.9546	3.2812	**85.1622**	$2.867.10^{-3}$	4.4446

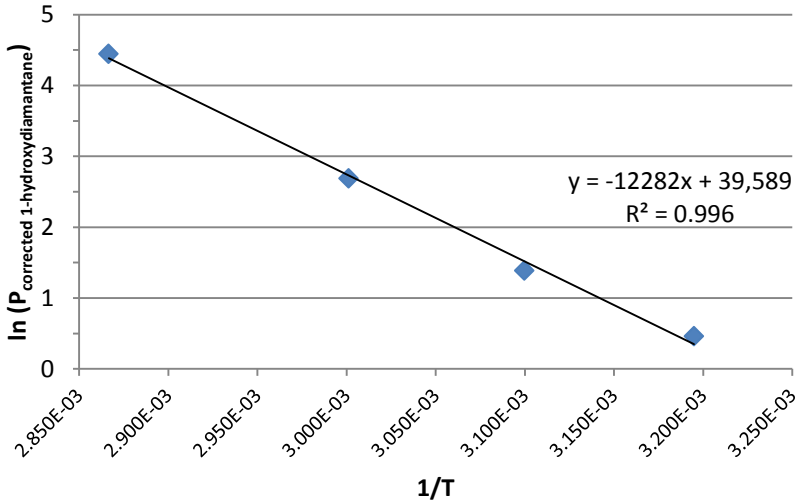

Figure 11S. Clausius-Clapeyron plot for 1-hydroxydiamantane

The enthalpy of sublimation of 1-hydroxydiamantane is ΔH = **102.1 ± 5** kJ/mol.

d) <u>4-Hydroxydiamantane</u>

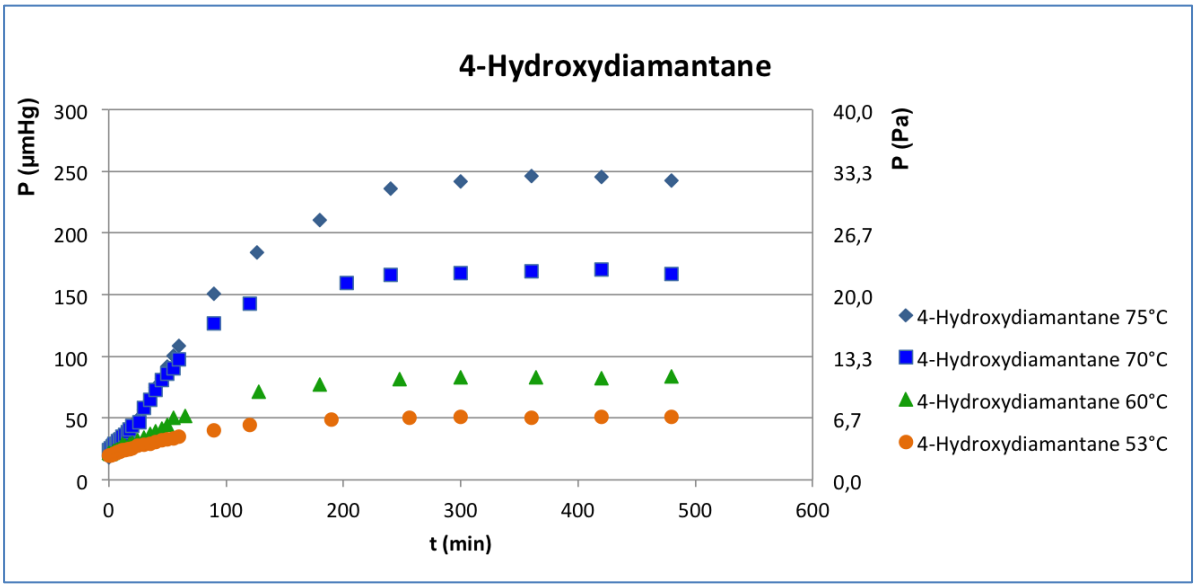

Figure 12S. Vapor pressure measurement for 4-hydroxydiamantane

Table 6S: Experimental vapor pressure and corrections for 4-hydroxydiamantane

T_{exp} (K)	P_{exp} (Pa)	P_{ref}/P ratio	$P_{corrected}$	1/T	ln ($P_{corrected}$)
326.05	6.7832	1.1211	**7.6048**	$3.067.10^{-3}$	2.0288
331.55	11.0654	1.4526	**16.0740**	$3.016.10^{-3}$	2.7772
343.55	22.4611	2.5563	**57.4182**	$2.911.10^{-3}$	4.0504
348.20	32.5052	3.1823	**103.4402**	$2.872.10^{-3}$	4.6390

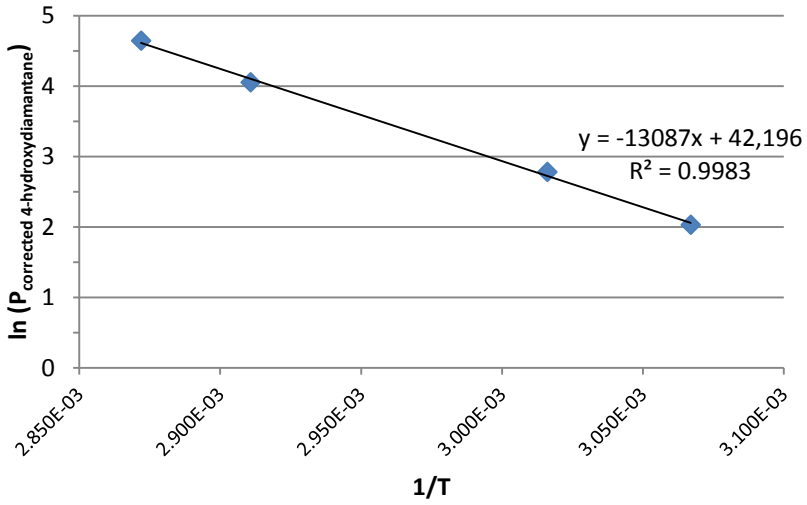

Figure 13S. Clausius-Clapeyron plot for 4-hydroxydiamantane

The enthalpy of sublimation of 4-hydroxydiamantane is ΔH = **108.8 ± 5** kJ/mol.

e) 4-Fluorodiamantane

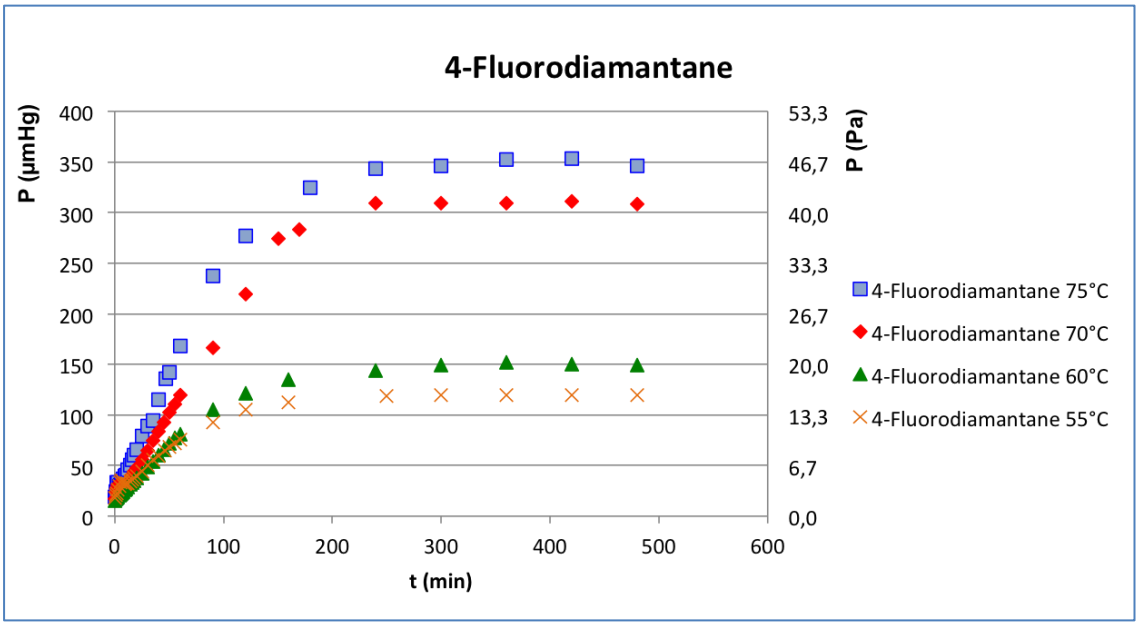

Figure 14S. Vapor pressure measurement for 4-fluorodiamantane

Table 7S: Experimental vapor pressure and corrections for 4-fluorodiamantane

T_{exp} (K)	P_{exp} (Pa)	P_{ref}/P ratio	**$P_{corrected}$**	1/T	ln ($P_{corrected}$)
327.65	15.9360	1.2089	**19.2646**	$3.052.10^{-3}$	2.9583
332.60	20.0234	1.5263	**30.5613**	$3.007.10^{-3}$	3.4197
343.65	41.2146	2.5684	**105.8562**	$2.910.10^{-3}$	4.6621
348.55	46.6133	3.2352	**150.8014**	$2.869.10^{-3}$	5.0160

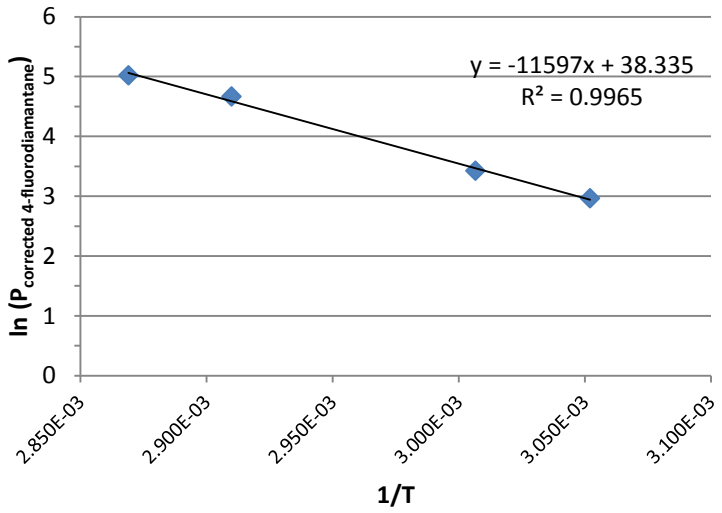

Figure 15S. Clausius-Clapeyron plot for 4-fluorodiamantane

The enthalpy of sublimation of 4-fluorodiamantane is ΔH = **96.4** ± **5** kJ/mol.

3) Vapor Deposition Conditions and Apparatus

a) Deposition at atmospheric pressure or low vacuum

A sublimation apparatus was designed for running vapor deposition of NDs at atmospheric pressure on various supports (**Figure 16S**). Diamondoids for sublimation were placed in a DSC aluminum cup on a boron nitride element. Above this system was placed a planar substrate on which the diamondoids vapor will re-condense. Substrate and diamondoids were separated by a spacer of tunable size in ceramic. A boron nitride element was used as a heating element and was attached to a copper holder with tungsten clips in its corners. A thermocouple type K was fixed to a hole on the side of holder to get the approximate temperature of the heating element measured with a multimeter apparatus. The heating element itself was connected to the power supply. The power supply was tuned based on its voltage and current. The heating was obtained by the Joule effect by means of a generator and the temperature was monitored using a multimeter equipped with a thermocouple. For a given intensity the temperature of the system is higher under vacuum than under atmospheric air or argon. The system was sealed using copper gasket and a valve. It was connected to a vacuum ramp/argon, itself connected to a vane pump. Vacuum was measured with a vacuum manometer (± 1 mmHg). The work atmosphere was either air, argon or a primary vacuum was established (5 mbar). Whatever the atmosphere in the chamber, a pump cycle was operated for a period of 10 min. Depending on the conditions the valve was closed to achieve a static vacuum, or the vacuum ramp was used for slow introduction of argon. Then, the valve was closed for establishing a static atmosphere, or the valve remained open for dynamic vacuum operating conditions. After adjusting the intensity of the applied current the deposition could start. The temperature setting was also monitored as a function of time. After the deposition time, the source was switched off allowing the system to cool. Once the temperature dropped below 30 °C, the system was opened, the substrate on which the deposit was made was

characterized by optical microscopy and by scanning electron microscopy (SEM), EXD and additionally X-ray diffraction. To avoid tampering of the sample, it was stored sealed in a freezer at 4 °C.

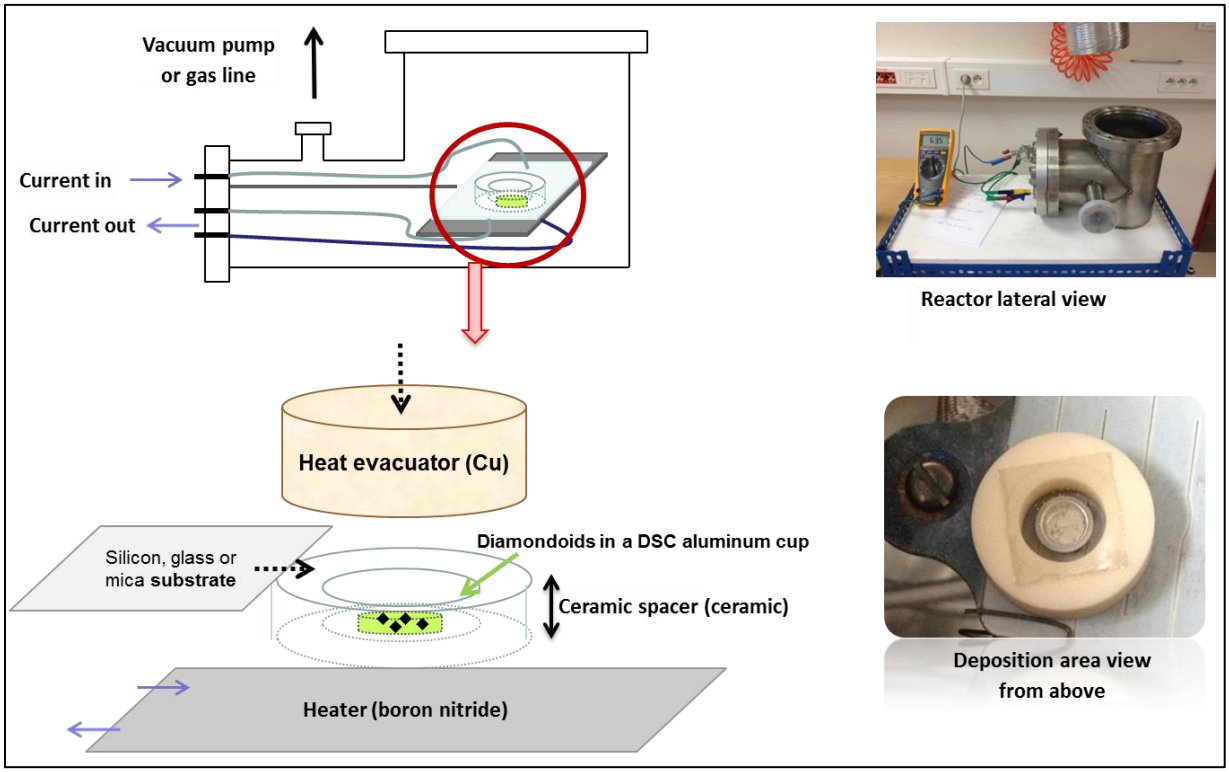

Figure 16S. Reactor for vapor deposition of diamondoids under controlled atmosphere

The substrates we used were cleaved mica, or silicon (111) from wafers. The substrates were placed on the top of the spacer. Deposits of diamondoids were achieved following various conditions (*vide infra* part 3), and all deposits were observed by optical microscopy (X16 to X500 size) before SEM analysis.

b) Vapor deposition apparatus for experiments under high vacuum (PVD)

Before exposure, silicon substrates Si(111) wafer pieces, *ca.* 1 cm^2, were cleaned out of carbon residue according to a RCA process (*Radio Corporation of America* is a standard set of wafer cleaning steps for high-temperature processing steps (*oxidation, diffusion, CVD,*

PVD, etc.) of silicon wafers in semiconductor manufacturing: *i*) the silicon was immersed in a solution of distilled water: NH_4OH : H_2O_2 = 5 : 1 : 1 at 75-80°C for 10 min; *ii*) it was then immersed in a solution of HF: distilled water = 1:100 or 1:50 at 25°C for 15 s; *iii*) the silicon wafer was immersed in a solution of distilled water/HCl/H_2O_2 = 5:1:1 at 75-80°C for 10 min; *iv*) the substrate was submersed in distilled water and dried with argon flushed when it was put inside the main chamber. Following a fast entry procedure, the treated Si substrates were introduced in a first chamber, mainly built in silica and insuring a low pressure of *ca.* 10^{-7} Pa (10^{-9} mbar). At this stage a small layer of amorphous SiO_2 inevitably forms at surface (as confirmed by XPS in **Figure SXPS1**). The wafers were heated at 800 °C by an induction oven for 12 min to complete the surface cleaning. Such treatment allowed removal of remaining contaminants such as atmospheric carbon and oxygen species. After cooling, the substrate was transferred in the deposition chamber that was previously baked out and maintained under vacuum with a turbo pump and an ionic pump. The diamondoids were held in a silica ampoule that was independently evacuated at room temperature for purification. The ampoule was connected to the deposition chamber through a stainless steel pipe. Through a linear translator, the pipe can reach up to 3 cm the silicon surface. During exposure, the ampoule and the pipe are heated at 80 °C or more with the help of a heater tape and a thermocoax wire in order to generate a *ca.* 10^{-1} Pa (10^{-3} mbar) partial pressure of diamondoids inside the ampoule which also avoids cold spots. Diamondoid vapors were then introduced into the vacuum chamber via a leak valve to control the pressure. During exposures, the silicon sample was kept at a temperature below 40 °C controlled by a thermocouple. During exposure, the pressure in the chamber increased slowly from 3.5 x 10^{-5} Pa up to 1.5 x10^{-4} Pa for exposure times longer than 15 min. A third chamber, connected to the two other ones, allows recording *in-situ* X-ray photoelectron spectroscopy (XPS in **Figure SXPS2** as example) spectra, using a VG Microtech CLAM4 MCD analyzer system. These experiments

were carried out with a non-monochromatised Al Kα radiation with detection normal to the surface.

Figure SXPS1. XPS of Si wafer surface after RCA protocol and 800 °C heating.

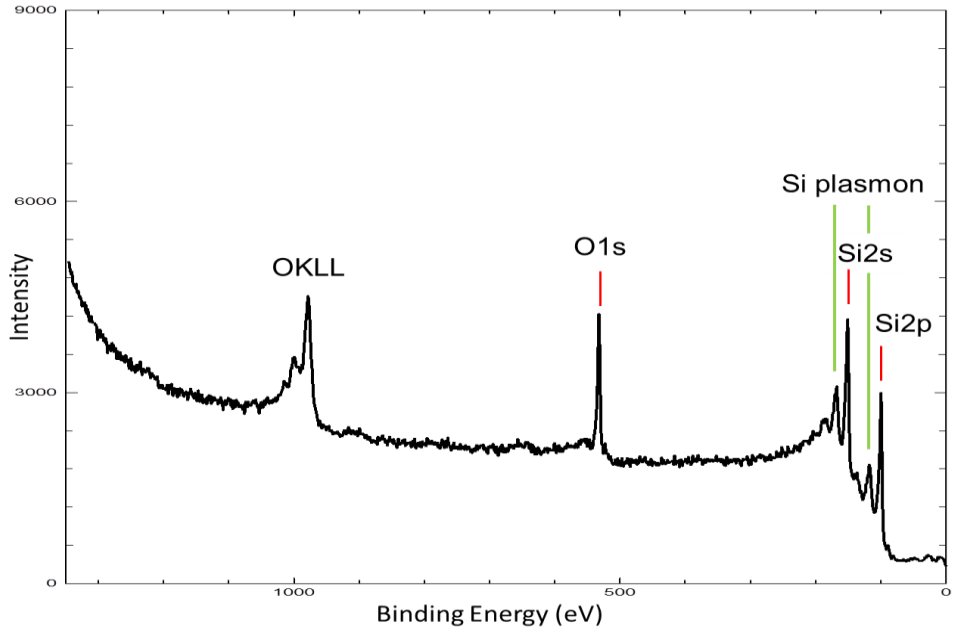

BE_{OKLL} = 978.3 eV, **BE_{O1s} = 532.5 eV**, $BE_{Si\ plasmon}$ = 167.8 eV, **BE_{Si2s} = 150.8 eV**, $BE_{Si\ plamon}$ = 117.7 eV, **BE_{Si2p} = 99.7 eV**)

Figure SXPS2. XPS of 1-hydroxydiamantane 3 deposited by PVD on Si(111)/SiO_2.

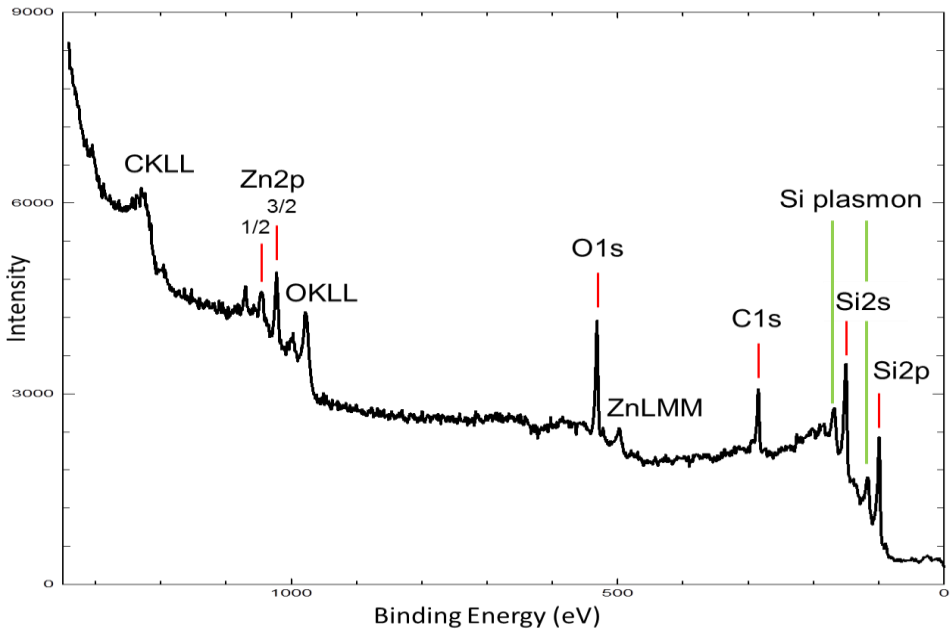

BE_{CKLL} = 1229.7 eV, $BE_{Zn2p1/2}$ = 1045.4 eV, $BE_{Zn2p3/2}$ = 1022.4 eV, BE_{OKLL} = 978.3 eV, **BE_{O1s} = 531.5 eV**, BE_{ZnLMM} = 498.4 eV, **BE_{C1s} = 284.0 eV**, $BE_{Si\ plasmon}$ = 167.8 eV, **BE_{Si2s} = 150.8 eV**, $BE_{Si\ plamon}$ = 117.7 eV, **BE_{Si2p} = 99.7 eV**). Zinc contamination in the substrate was detected.

Enhancement of interest from Figure SXPS1

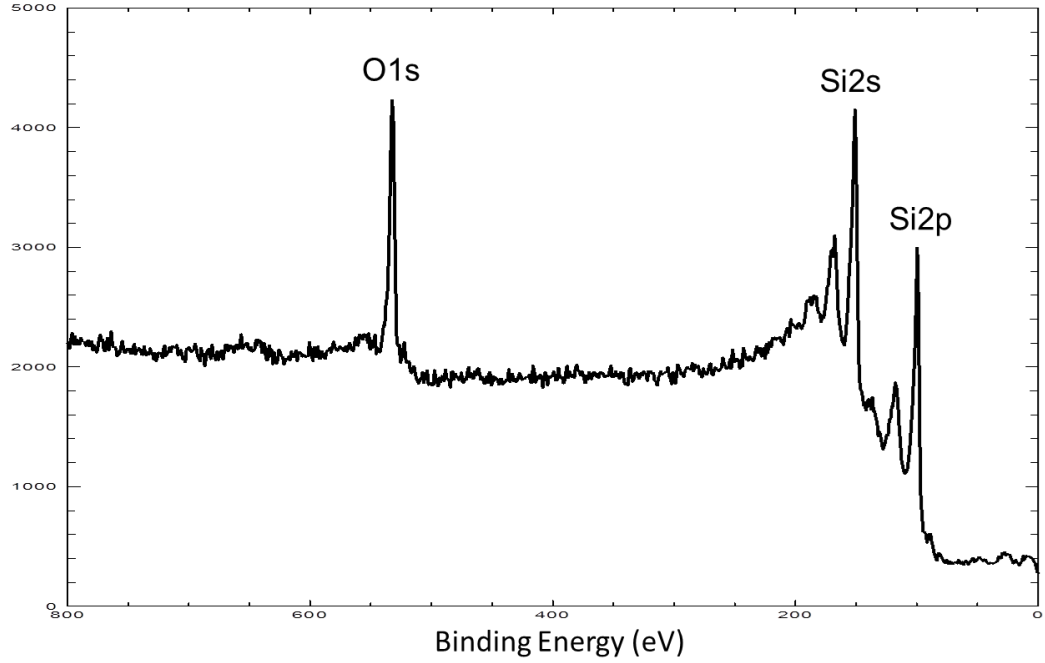

Enhancement of Interest from Figure SXPS2

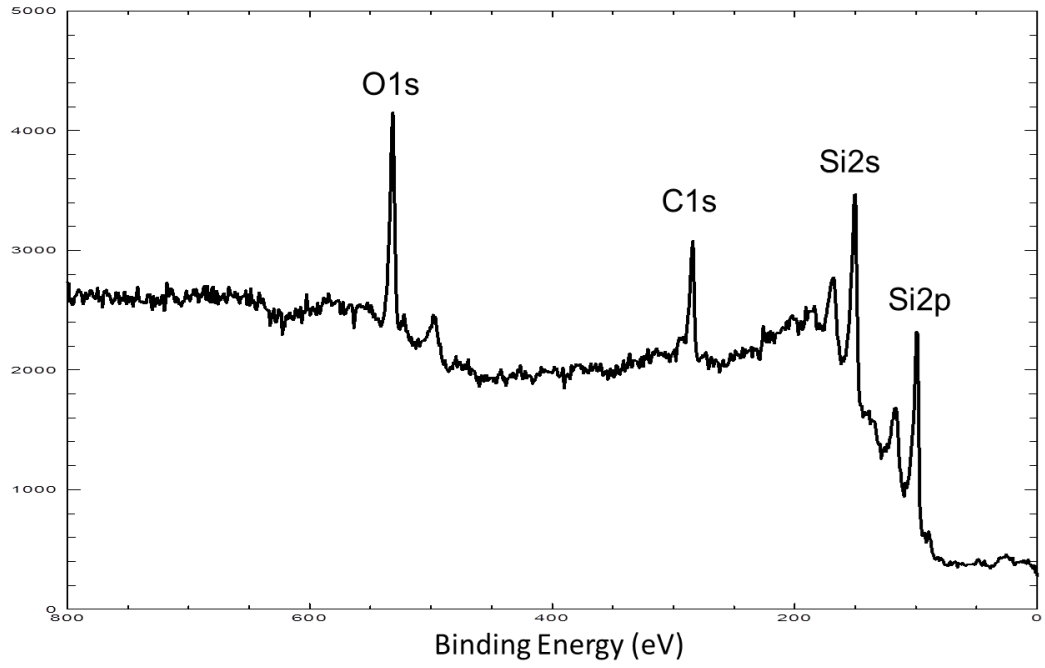

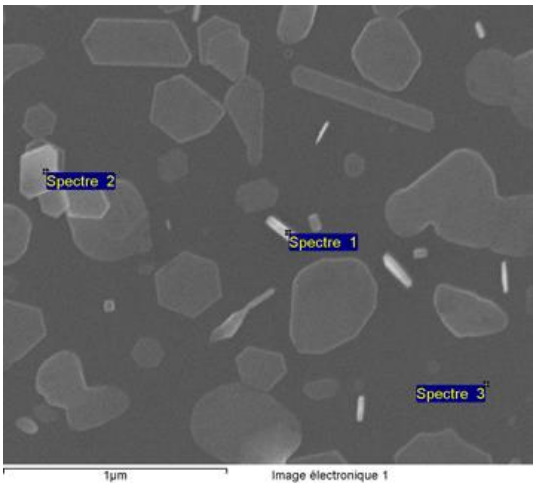

Analyzed Elements (Normalized) : % wt

	C	O	Si
Spectre 1	13.15	1.95	84.90
Spectre 2	13.72	2.20	84.08
Spectre 3	28.94		71.06
Max.	28.94	2.20	84.90
Min.	13.15	1.95	71.06

Figure SEDX1. EDX quantitative analysis of 1-hydroxydiamantane 3 deposited by PVD on Si

4) Optical Microscopy of Crystal Deposits from Vapor Deposition of Diamondoids

a) Adamantane deposit

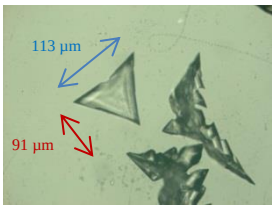

Mica: 50°C, 30 min(200x)

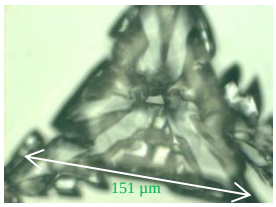

Silicon without evacuator: 0.8A, 40 min(500x)

b) 1–Hydroxyadamantane deposit

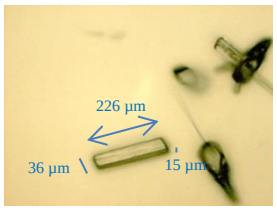

Mica, 50°C, 30 min: 100x

200x

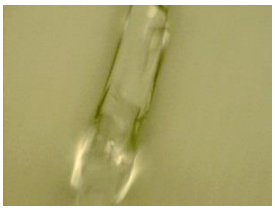

500x

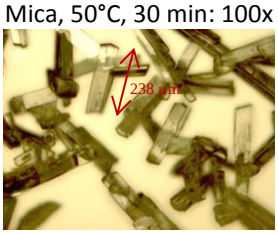

Mica, 85°C, 30 min: 100x

200x

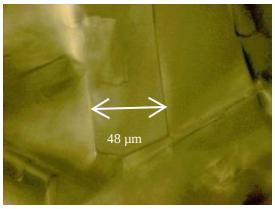

500x

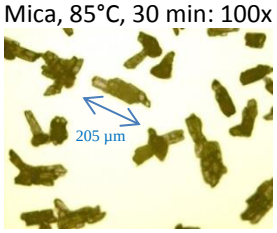

Silicon, 80°C, 30 min: 100x

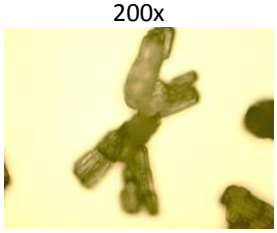

200x

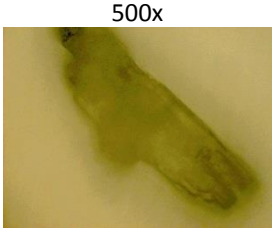

500x

c) *Adamantyl diphenylphosphinite deposit*

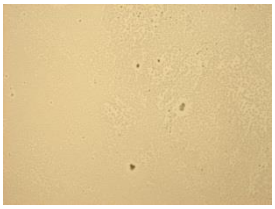
Mica, 85°C, 30 min: 100x

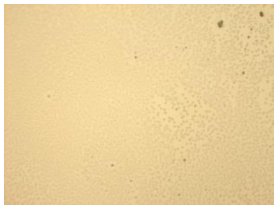
200x

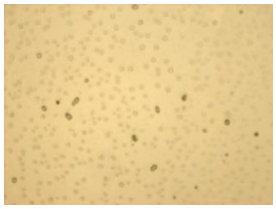
500x

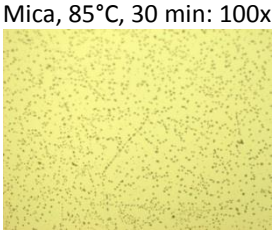
Silicon, 80°C, 30min: 100x

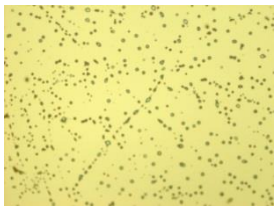
200x

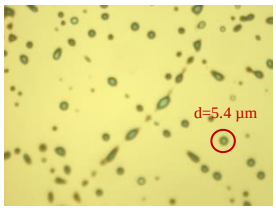

500x

d) *Aminoadamantane deposit*

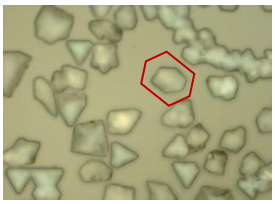
Mica, 50°C, 30 min: 100x

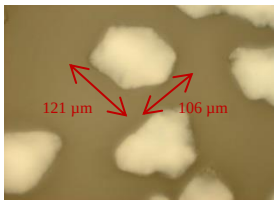

200x

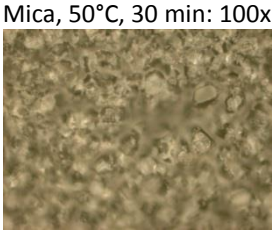
Mica, 85°C, 30 min: 100x


200x

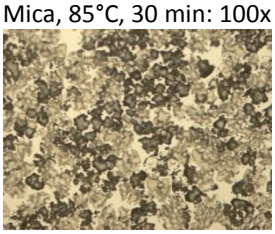
Silicon, 80°C, 30min: 100x

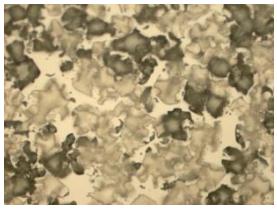
200x


500x

e) *Diamantane deposit*

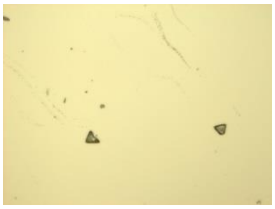
Mica, 50°C, 30 min: 100x


200x

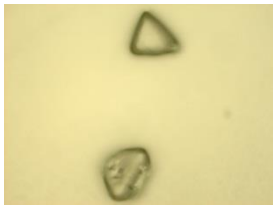
500x

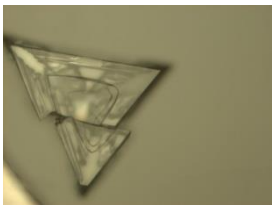
Mica, 50°C, 16 h: 100x

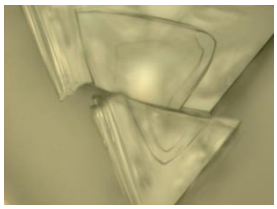
200x


500x

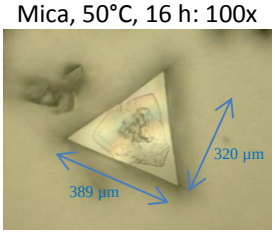

Mica, 85°C, 30 min: 100x

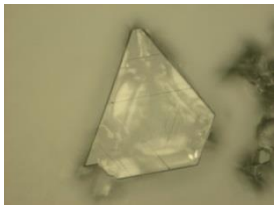
200x


500x

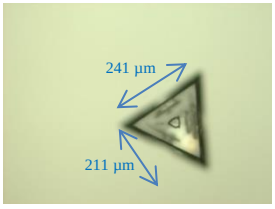

Silicon, 80°C, 30min: 100x

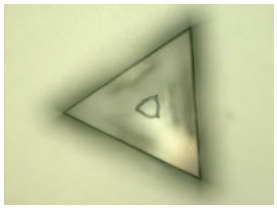
200x


500x

f) *1-Hydroxydiamantane deposit*


Mica, 50°C, 30 min: 100x


200x


500x

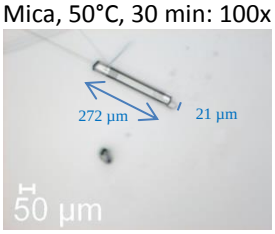

Mica, 50°C, 16 h: 100x

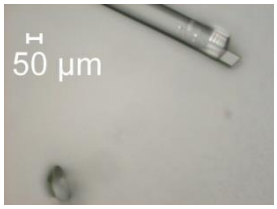

200x


500x

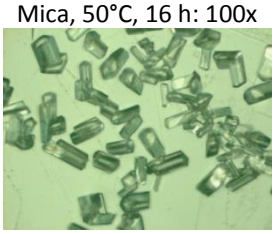
Mica, 85°C, 30 min: 100x

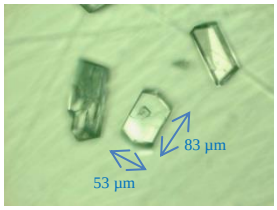

200x

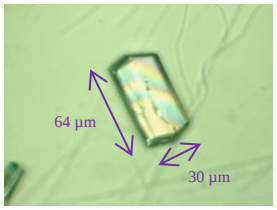

500x

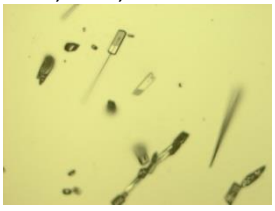
Silicon, 80°C, 30min: 100x

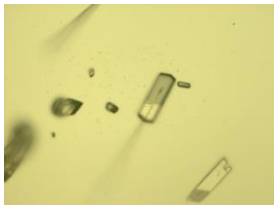
200x

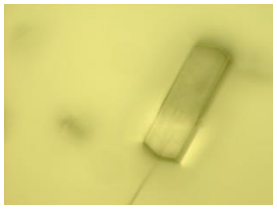
500x

g) *4-Hydroxydiamantane deposit*

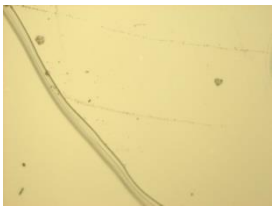
Mica, 50°C, 30 min: 100x

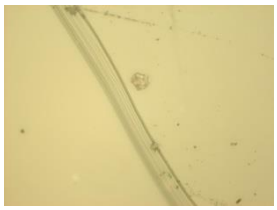
200x

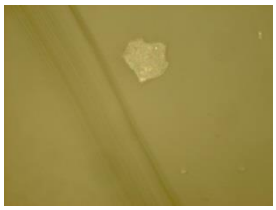
500x

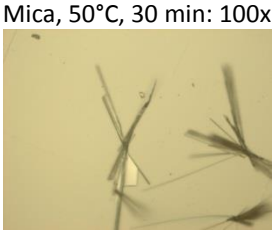
Mica, 50°C, 16 h: 100x

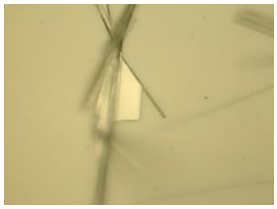
200x


500x

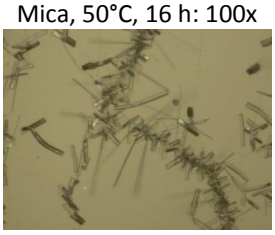
Mica, 85°C, 30 min: 100x

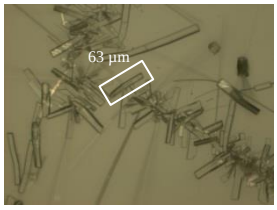

200x


500x

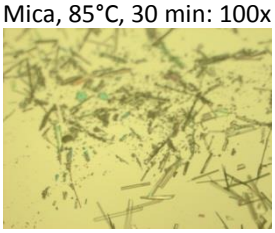
Silicon, 80°C, 30min: 100x

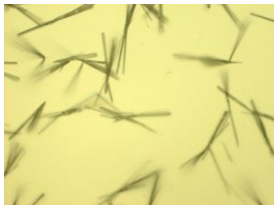
200x


500x

h) *4,9-Dihydroxydiamantane deposit*

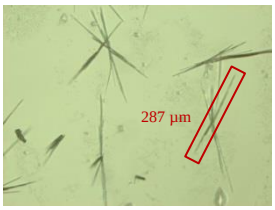

Mica, 85°C, 40 min: 100x

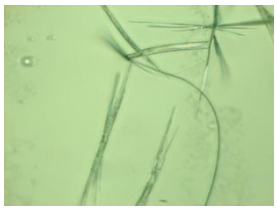
200x

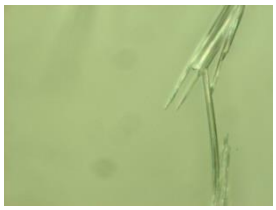
500x

i) *4-Fluorodiamantane deposit*

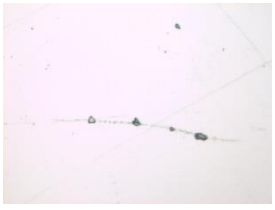
Mica, 50°C, 30 min: 100x


200x


500x

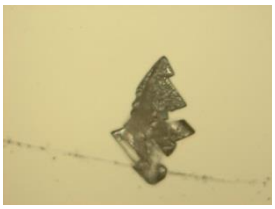
Mica, 50°C, 16 h: 100x

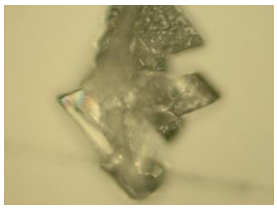
200x

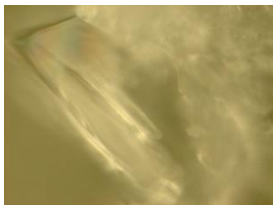
500x

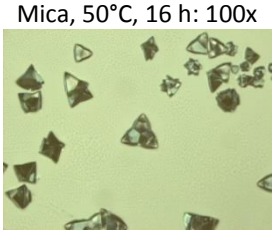

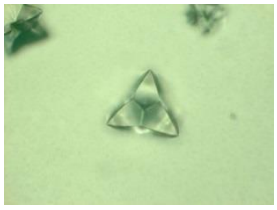

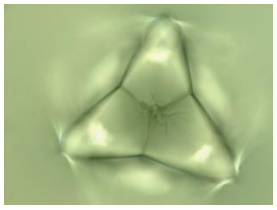

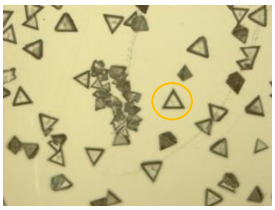

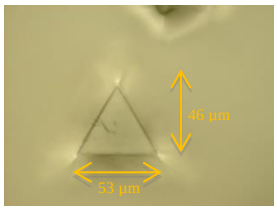

Mica, 85°C, 30 min: 100x 200x 500x

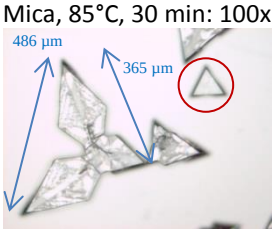

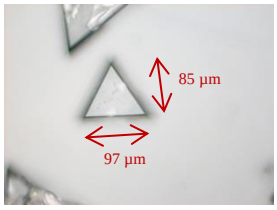


Mica, 85°C, 32 min: 100x 200x 500x

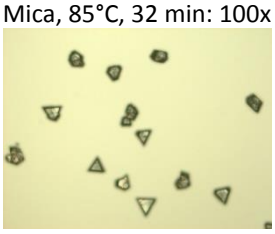

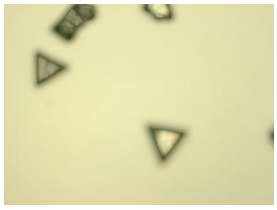

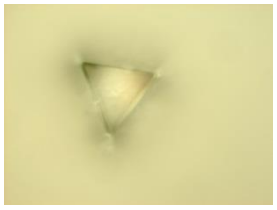
Silicon, 80°C, 30min: 100x 200x 500x

j) *4,9-Difluorodiamantane deposit*


Mica, 50°C, 30 min: 100x

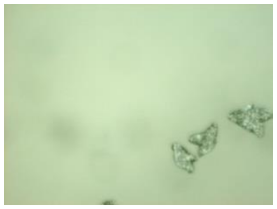
500x

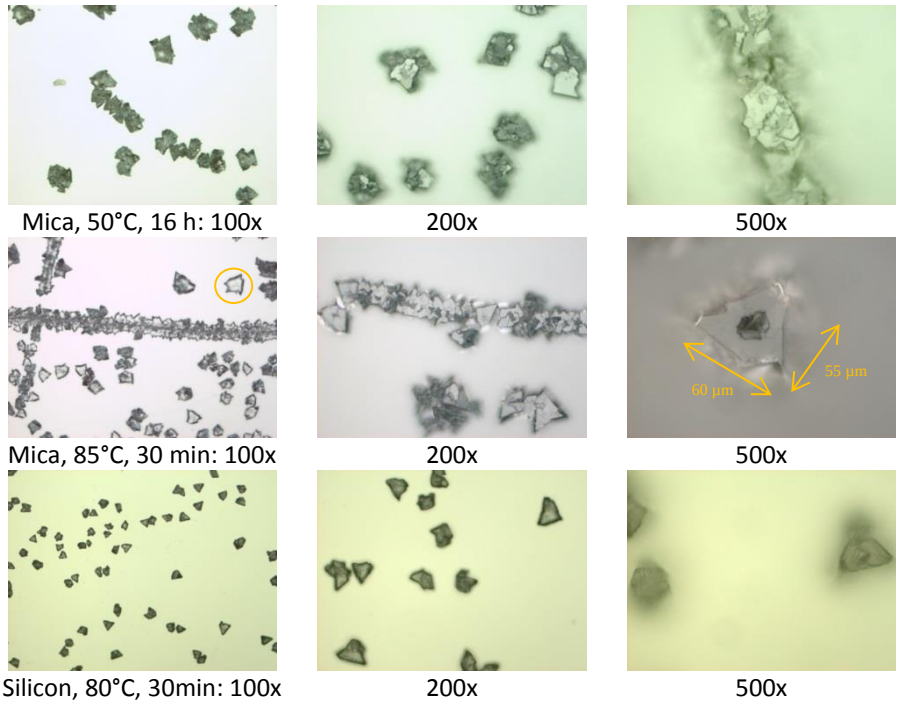

5) Control of crystallinity from X-Ray diffraction studies

To better assess the crystallinity of the deposit suggested by microscopy we performed X-Ray diffraction analysis on the deposits. For instance, using self-assembly of 1-hydroxydiamantane **3** achieved by our vapor deposition process, a single crystal diffraction analysis was successfully achieved, confirming the structure of this diamondoid that has been recently reported.[8] As shown in the Ortep **Figure 17S**, the X-Ray of 1-hydroxydiamantane **3** reveal a structure in which four diamondoid molecules are arranged in a special way, where they are connected through a four members loop with hydrogen bonding.

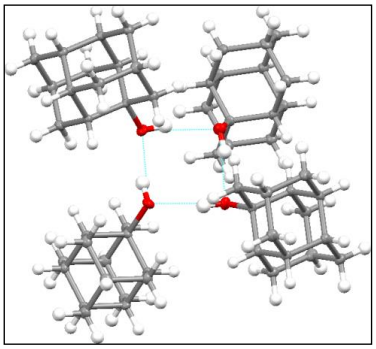

Figure 17S. Molecular structure and unit cell arrangement of 1-hydroxydiamantane 3 from X-ray diffraction of a microcrystal deposited by vapor deposition.

6) Deposits from Solution Dip Coating of Functionalized-Diamondoids

For dip coating a silicon wafer (decarbonized Si(111) with an amorphous SiO_2 layer at surface) 1x1 cm^2 was dipped into a 1 mL solution of dichloromethane containing 10 mg of diamondoids for 10 s. The silicon wafer was removed vertically slowly by using clean and dry small pliers. The sample was let dried for several hours under air inside a desiccator. As confirmed by optical microscopy no specific crystalline self-assembly was obtained in each case.

Optical Microscopy and Scanning Electron Microscopy (SEM)

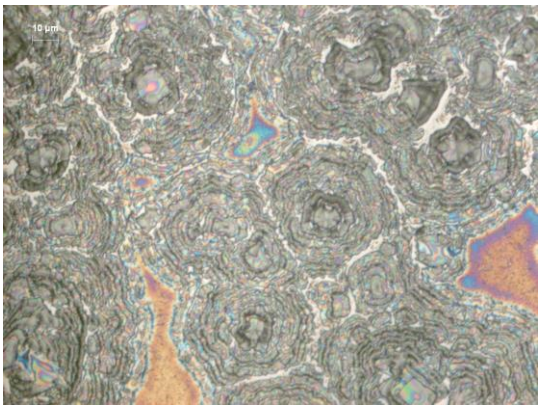

Optical microscopy of 1-adamantyldiphenyl thiophosphinite on silicon by dip coating from CH_2Cl_2 solution

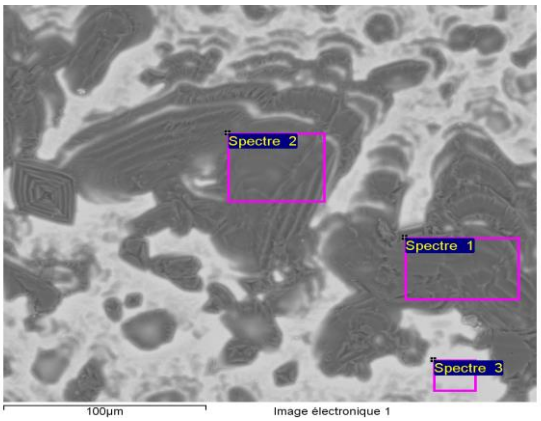

SEM image of 1-adamantyldiphenyl thiophosphinite on silicon by dip coating from CH_2Cl_2 solution

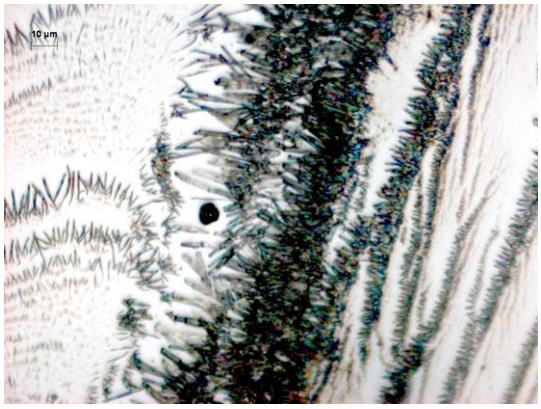

Optical microscopy of 4,9-dihydroxydiamantane on silicon by dip coating from CH_2Cl_2 solution

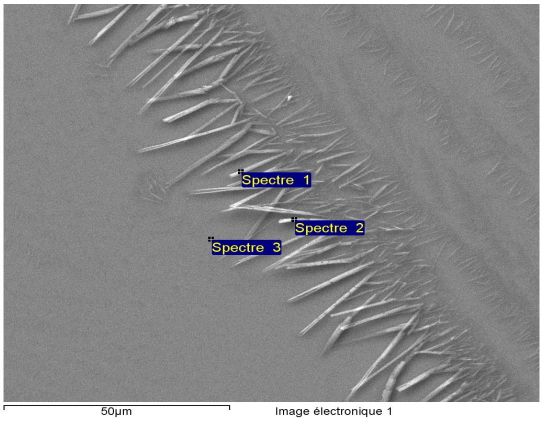

SEM image of 4,9-dihydroxydiamantane on silicon by dip coating from CH_2Cl_2 solution

References

[1] J. S. Chickos, W. E. Acree, Jr. *J. Phys. Chem. Ref. Data*. **2002**, *31*, 1910.

[2] A. S. Carson, P. G. Laye, W. V. Steele, D. E. Johnston, M. A. McKervey, *J. Chem. Thermodyn.* **1971**, *3*, 915.

[3] C. A. Fyfe, D. Harold-Smith. *J. Chem. Soc. Faraday Trans. II*. **1974**, 967.

[4] T. Clark, T. Knox, H. Mackle, M. A. McKervey, J. J. Rooney. *J. Chem. Soc. Faraday Trans. I*. **1975**, *71*, 2107.

[5] (a) T. Clark, T. Knox, M. A. McKervey, H. Mackle, J. J. Rooney, *J. Am. Chem. Soc*. **1979**, *101*, 2404; (b) T. Clark, T. Knox, M. A. McKervey, H. Mackle, *J. Chem. Soc. Perkin Trans.* 2. **1980**, 1686.

[6] M. H. Keshavarz, M. Zamani, F. Atabaki, K. H. Monjezi. *Comp. Theor. Chem.*, **2013**, *1006*, 105.

[7] C. G. De Kruif, T. Kuipers, J. C. V. Miltenburg, R. C. F. Schaake, G. Stevens. *J. Chem. Thermodynamics.* **1981**, *13*, 1081.

[8] C. Y. Yu, Q. Li, L. B. Wang, H. W. Ma, *Acta Cryst., E: Structure Reports Online*. **2006**, *62*, o2369.